Wärme- und Stoffübertragung 20, 189–201 (1986)

Wärme- und Stoffübertragung

Development of a turbulent near-wall temperature model and its application to channel flow

H. Akbari, A. Mertol, A. Gadgil, R. Kammerud, and F. Bauman, Berkeley, CA, USA

Abstract. A numerical study of fluid flow and heat transfer in a two-dimensional channel under fully developed turbulent conditions is reported. A computer program which is capable of treating both forced and natural convection problems under turbulent conditions has been developed. The code uses the high-Reynolds-number form of the two equation turbulent model ($k-\varepsilon$) in which a turbulent kinetic energy near-wall model is incorporated in order to accurately represent the behavior of the flow near the wall, particularly in the viscous sublayer where the turbulent Reynolds number is small. A near-wall temperature model has been developed and incorporated into the energy equation to allow accurate prediction of the temperature distribution near the wall and, therefore, accurate calculation of heat transfer coefficients.

The sensitivity of the prediction of flow and heat transfer to variations in the coefficients used in the turbulence model is investigated. The predictions of the model are compared to available experimental and theoretical results; good agreement is obtained. The inclusion of the near-wall temperature model has further improved the predictions of the temperature profile and heat transfer coefficient. The results indicate that the turbulent kinetic energy Prandtl number should be a function of Reynolds number.

Entwicklung eines turbulenten, wandnahen Temperaturmodells und seine Anwendung auf Kanalströmung

Zusammenfassung. Es wird über eine numerische Studie der Strömung und des Wärmetransportes in einem zweidimensionalen Kanal mit voll entwickelter Turbulenz berichtet. Ein Computerprogramm wurde entwickelt, das in der Lage ist, sowohl Zwangs- als auch Naturkonvektion unter turbulenten Bedingungen zu behandeln. Das Programm verwendet die „High-Reynolds-Number"-Form des turbulenten Zweigleichungsmodells ($k-\varepsilon$-Modell) in das ein Ansatz für die wandnahe, turbulente, kinetische Energie eingearbeitet ist, um das Verhalten der Strömung nahe der Wand genau wiederzugeben, insbesondere in der viskosen Unterschicht, wo die turbulente Reynolds-Zahl klein ist. Es wurde ein wandnahes Temperaturmodell entwickelt und in die Energiegleichung eingearbeitet, um eine genaue Vorhersage der Temperaturverteilung nahe der Wand zu ermöglichen und damit die Wärmeübergangskoeffizienten genau zu berechnen.

Die Empfindlichkeit für die Vorhersage der Strömung und der Wärmeübertragung auf Veränderungen in den Koeffizienten des verwendeten Turbulenzmodells wird untersucht. Die Vorhersagen des Modells werden mit verfügbaren experimentellen Daten und theoretischen Ergebnissen verglichen. Es wurde gute Übereinstimmung erzielt. Die Einbeziehung des wandnahen Temperaturmodells brachte weitere Verbesserung der Vorhersage des Temperaturprofils und des Wärmeübergangskoeffizienten. Die Ergebnisse zeigen, daß die turbulente, kinetische Prandtl-Zahl eine Funktion der Reynolds-Zahl sein sollte.

Nomenclature

A	empirical coefficient, Eq. (27)
b	channel width
c_l	constant of proportionality between length scale l and distance from wall (applied over near-wall cell) = 2.55, Eq. (17)
$C_1, C_2, C_{\mu\infty}$	constants in the $k-\varepsilon$ turbulent model, Eq. (8)
c_p	specific heat
E^*	constant in logarithmic velocity profile = 5.0, Eq. (12)
k	turbulent kinetic energy
K	empirical coefficient, Eq. (27)
l_m	mixing length
Nu	Nusselt number, Eq. (19)
p	pressure
Pr	Prandtl number $= \nu/\alpha$
Re	Reynolds number $= v_m b/2\nu$
Re_t	turbulent Reynolds number, Eq. (10)
Re_v	viscous sublayer Reynolds number $= y_v k_v^{1/2}/\nu = 20.0$
$\overline{Re}$	average Reynolds number
t	time
T	temperature
u	velocity in x-direction
v	velocity in y-direction
x	horizontal coordinate; main flow direction
y	vertical coordinate

Greek symbols

α	thermal diffusivity
ε	dissipation rate of turbulence energy
κ	von Karman constant = 0.4187
κ^*	constant in logarithmic velocity profile $= \kappa C_{\mu\infty}^{1/4} = 0.23$
λ	thermal conductivity
μ	laminar dynamic fluid viscosity
μ_t	turbulent dynamic fluid viscosity
ν	laminar kinematic fluid viscosity
ϱ	density
σ_k	turbulent kinetic energy Prandtl number
σ_t	turbulent temperature Prandtl number
σ_ε	turbulent dissipation Prandtl number
τ	shear stress

Subscripts

b	bulk
c	cold
e	edge of near-wall cell
E	center of cell adjacent to the near-wall cell
h	hot
m	maximum of experimental value
P	center of near-wall cell
t	turbulent
v	edge of viscous sublayer
w	wall

1 Introduction

Several different models have been developed to predict turbulent flow. Among them the two-equation $k-\varepsilon$ model has attracted considerable attention. Although the model was originally developed for high-Reynolds-number boundary layer flows [1], it has been extended to include the prediction of turbulent flow at low Reynolds numbers as well [2, 3]. Both the high- and low-Reynolds-number forms of the $k-\varepsilon$ model have been successful in predicting aspects of turbulent flow in many cases. The high-Reynolds-number form of the model has attracted more attention because it reduces the computation time and storage. However, this is sometimes accomplished by a degradation in accuracy in predicting flow near boundaries where the Reynolds number is small. To account for the low-Reynolds-number region near the wall, the high-Reynolds-number $k-\varepsilon$ model equations have been modified to include a near-wall representation for turbulent kinetic energy [4]. The inclusion of this near-wall model also allows empirical relations to be implemented for special purposes, e.g., an empirical relation for wall roughness. Recently, the near-wall kinetic energy model has been modified by dividing the near-wall region into viscous, buffer and fully turbulent regions and improved agreement with experimental data has been obtained [5].

The $k-\varepsilon$ model has been used extensively to predict turbulence in forced flow problems. Chieng and Launder [4] and Johnson and Launder [6] have used the high-Reynolds-number form of the model to predict the flow downstream of an abrupt pipe expansion. Sindir [7–10] has compared the predictions of different turbulent flow models for a sudden expansion in a channel. Humphrey and Pourahmadi [11] and Humphrey and Chang [12] have used the $k-\varepsilon$ model to study the flow in a curved channel. Naot and Rodi [13] have used the model for predictions on the secondary currents in channel flow. The application of the $k-\varepsilon$ model to different problems has shown that the parameters in the model are not universal; improved agreement with experimental data is obtained if some of the parameters in the original $k-\varepsilon$ model equations are allowed to vary with the Reynolds number [14].

In most previous studies of the $k-\varepsilon$ model, for purposes of validation, predictions of the model have been compared to the experimental data of simple Simple flow configurations lend themselves more eas experimental techniques, and data thus produced a more suitable for verification of the theoretical models and/or evaluation of prediction methods. Fully developed channel and pipe flows are examples for which experimental data exists covering the important parameters of interest.

Most of the aforementioned studies have concentrated on comparison of the hydrodynamics of the flow (i.e. velocity, turbulent kinetic energy, etc.) with the experimental data. For the heat transfer aspects of the problem, only heat transfer coefficients have been used for comparison purposes. However, the velocity and turbulent kinetic energy profiles alone are not enough to provide a complete validation of the model in non-isothermal flow. For this purpose the temperature and eddy diffusivity profiles must also be compared to the experimental data. While it is relatively easy to adjust the $k-\varepsilon$ model constants to predict the velocity and the turbulent kinetic energy profiles fairly well, it will be shown in the present study that, for these same model constants, the temperature and turbulent viscosity predictions can differ greatly from the experimental values.

In the present work, the high-Reynolds-number form of the two-equation $k-\varepsilon$ turbulent model has been used along with a slight variation of the previously developed turbulent kinetic energy near-wall physical model [4]. A sensitivity study of the $k-\varepsilon$ model constants has been performed to select the best set of constants for the flow and heat transfer predictions in a channel. To improve the predictions of the temperature and heat transfer coefficients, a near-wall model for temperature has been developed. With the inclusion of both near-wall models, the predictions of all dependent variables have shown better agreement with experimental data. The results have also indicated that the turbulent viscosity variation is highly dependent on the choice of turbulent kinetic energy Prandtl number.

The predictions of the model have been compared to the experimental data of fully developed turbulent channel flow. The previous experimental and theoretical studies of turbulent channel flow, other than the ones mentioned above, will be discussed separately below.

1.1 *Experimental studies*

In an early experimental study, Washington and Mark [15] measured heat transfer and pressure drop in rectangular air passages. For fully turbulent flow ($\overline{Re} > 13000$) they presented equations for the friction factor and Nusselt number. Corcoran et al. [16, 17] and Page et a [18, 19] performed heat transfer and fluid flow measurements for turbulent flow between two parallel plates an determined the temperature and velocity as a function position in the channel. Laufer [20] made mean-speed an

axial-fluctuation measurements within the laminar sublayer of a two-dimensional turbulent channel flow at different Reynolds number. The distribution of streamwise velocity fluctuations showed that the influence of the viscosity extended farther from the wall than indicated by the mean velocity profile. It was also found that the dimensionless mean fluctuating quantities (e.g., velocities) decreased with an increasing Reynolds number. Clark [21] performed similar measurements in the viscous sublayer by using constant-temperature hot-wire anemometry. Frequency spectral of the fluctuating velocity components were obtained and the mean velocity distribution in the sublayer was determined to produce a reasonable estimate of skin friction. Hussain and Reynolds [22] performed measurements in a channel with fully developed turbulent air flow and presented experimental streamwise and mean turbulent velocity distributions, frequency spectra, and calculated eddy viscosity distributions. El Telbany and Reynolds [23, 24], in their experiments with a flat channel having one wall movable relative to the other, measured the velocity distribution and turbulence (longitudinal, normal and lateral velocity fluctuation intensities) in plane turbulent flow established by the various combinations of pressure gradient and wall velocities. They developed an empirical description for the viscous, logarithmic and gradient portions of the wall layers as well as the turbulence near the wall and in the turbulent core. It was also shown that the intensity of velocity fluctuations coalesced, to a reasonable approximation, when normalized with the appropriate length and velocity scales.

Most of the above-mentioned experimental work has dealt with the measurements of hydrodynamic quantities. Only Corcoran et al. [16, 17] and Page et al. [18, 19] report temperature measurements. Heat transfer related results of the other experiments are limited to presenting the general behavior of the temperature gradient close to the wall, that is, the Nusselt number.

In addition to the aforementioned experiments, other studies have emphasized heat transfer coefficients. Lancet [25] studied the effect of surface roughness on the heat transfer coefficient for fully developed turbulent flow in ducts with uniform heat flux; the results indicated that rough channel surfaces appreciably increase heat transfer and friction coefficients. Levy, Fuller and Niemi [26] compared their channel flow experimental data to predictions of several empirical equations for the Nusselt number which were developed for pipe flow. It was found that the heat transfer rates for channel flow are 15–30% below the values predicted by the circular pipe equations. It was also concluded that for the calculation of the Nusselt number, the empirical equations with the constant exponent on the Reynolds number are inadequate. Sparrow, Lloyd and Hixon [27] measured the heat transfer coefficients in an asymmetrical heated rectangular duct and compared their measurements with some analytical predictions for the parallel-plate channel.

1.2 Theoretical studies

Turbulent channel flow has been the subject of numerous theoretical studies. However, the more pertinent studies – those which address the velocity, temperature and turbulent viscosity profiles for fully developed (both velocity and temperature) channel flow – are scarce. By analogy between momentum and heat transfer, Martinelli [28] studied the heat transfer to molten metals for a constant wall temperature pipe flow and calculated the Nusselt number. A correlation for the heat transfer coefficient for channel flow was developed using the same methodology. Harrison and Menke [29] extended the work of Martinelli to obtain the Nusselt number for channel flow which was heated at one wall and adiabatic at the other. Seban [30] extended this work by studying heat transfer in fully developed channel flow with different wall temperatures. The results were condensed into a correlation to calculate the Nusselt number. Hatton and Quarmby [31, 32] obtained a general correlation for the calculation of the Nusselt number in turbulent flow between asymmetrically heated parallel plates. In preliminary work, Barrow [33] obtained correlations for the Nusselt number for turbulent flow between parallel plates with unequal heat fluxes. For fully developed flow under conditions where the heat added to the channel at one surface is fully removed at the other surface, it was found that the temperature varies linearly in the core region across the channel. In later theoretical and experimental work, Barrow [34] and Barrow and Lee [35] extended these results and modified the equation for the prediction of the Nusselt number. It was concluded that the heat transfer coefficient is a function of the heat flux distribution over the walls as well as of the Reynolds and the Prandtl numbers.

2 Analysis

The transport equations for turbulent flow in a channel are solved to determine the velocity and temperature profiles and the heat transfer coefficient. The form of the momentum equations in Ref. [7] is used. The two-dimensional conservation equations of the flow are given as follows:

(I) Continuity equation:

$$\frac{\partial \varrho}{\partial t} + \frac{\partial}{\partial x}(\varrho u) + \frac{\partial}{\partial y}(\varrho v) = 0 \tag{1}$$

(II) x-momentum equation:

$$\frac{\partial}{\partial t}(\varrho u) + \frac{\partial}{\partial x}(\varrho u^2) + \frac{\partial}{\partial y}(\varrho u v) = -\frac{\partial p}{\partial x} + \frac{\partial}{\partial x}\left[2(\mu + \mu_t)\frac{\partial u}{\partial x} - \frac{2}{3}\varrho k\right] + \frac{\partial}{\partial y}\left[(\mu + \mu_t)\left(\frac{\partial u}{\partial y} + \frac{\partial v}{\partial x}\right)\right]. \tag{2a}$$

(III) r-momentum equation:

$$\frac{\partial}{\partial t}(\varrho v) + \frac{\partial}{\partial x}(\varrho u v) + \frac{\partial}{\partial y}(\varrho v^2) = -\frac{\partial p}{\partial y} + \frac{\partial}{\partial x}\left[(\mu + \mu_t)\left(\frac{\partial v}{\partial x} + \frac{\partial u}{\partial y}\right)\right] + \frac{\partial}{\partial y}\left[2(\mu + \mu_t)\frac{\partial v}{\partial y} - \frac{2}{3}\varrho k\right] \quad (2b)$$

(IV) Energy equation:

$$\frac{\partial}{\partial t}(\varrho T) + \frac{\partial}{\partial x}(\varrho u T) + \frac{\partial}{\partial y}(\varrho v T) = \frac{\partial}{\partial x}\left[\left(\frac{\lambda}{c_p} + \frac{\mu_t}{\sigma_t}\right)\frac{\partial T}{\partial x}\right] + \frac{\partial}{\partial y}\left[\left(\frac{\lambda}{c_p} + \frac{\mu_t}{\sigma_t}\right)\frac{\partial T}{\partial y}\right]. \quad (3)$$

The effective turbulent viscosity, μ_t, is obtained from the k - ε model [1–4] which relates this viscosity to the turbulent kinetic energy and its dissipation rate. The high-Reynolds-number form of the equations has been used. Modifications to this form of the model are necessary to account for the low-Reynolds-number conditions encountered near the physical boundaries of the channel. The turbulent kinetic energy and its dissipation rate are calculated by using the following equations:

(I) Turbulent kinetic energy, k:

$$\frac{\partial}{\partial t}(\varrho k) + \frac{\partial}{\partial x}(\varrho u k) + \frac{\partial}{\partial y}(\varrho v k) = \frac{\partial}{\partial x}\left[\left(\mu + \frac{\mu_t}{\sigma_k}\right)\frac{\partial k}{\partial x}\right] + \frac{\partial}{\partial y}\left[\left(\mu + \frac{\mu_t}{\sigma_k}\right)\frac{\partial k}{\partial y}\right] + \mu_t\left[\left(\frac{\partial u}{\partial y} + \frac{\partial v}{\partial x}\right)^2 + 2\left(\frac{\partial u}{\partial x}\right)^2 + 2\left(\frac{\partial v}{\partial y}\right)^2\right] - \varrho\varepsilon. \quad (4)$$

(II) Dissipation rate of turbulent energy, ε:

$$\frac{\partial}{\partial t}(\varrho \varepsilon) + \frac{\partial}{\partial x}(\varrho u \varepsilon) + \frac{\partial}{\partial y}(\varrho v \varepsilon) = \frac{\partial}{\partial x}\left[\left(\mu + \frac{\mu_t}{\sigma_\varepsilon}\right)\frac{\partial \varepsilon}{\partial x}\right] + \frac{\partial}{\partial y}\left[\left(\mu + \frac{\mu_t}{\sigma_\varepsilon}\right)\frac{\partial \varepsilon}{\partial y}\right] + C_1\frac{\varepsilon}{k}\mu_t\left[\left(\frac{\partial u}{\partial y} + \frac{\partial v}{\partial x}\right)^2 + 2\left(\frac{\partial u}{\partial x}\right)^2 + 2\left(\frac{\partial v}{\partial y}\right)^2\right] - C_2\varrho\frac{\varepsilon^2}{k}. \quad (5)$$

The effective turbulent viscosity is calculated from

$$\mu_t = C_\mu \varrho k^2/\varepsilon \quad (6)$$

where

$$C_\mu = C_{\mu\infty} f_\mu. \quad (7)$$

The asymptotic, high-Reynolds-number values of the coefficients as suggested in [1, 2, 7] are [1]:

$$C_{\mu\infty} = 0.09, \quad C_1 = 1.44, \quad C_2 = 1.92, \quad \sigma_k = 1.0, \quad \sigma_t = 0.9, \quad \text{and} \quad \sigma_\varepsilon = 1.22. \quad (8)$$

In order to investigate the sensitivity of the $k-\varepsilon$ model predictions, three different forms for f_μ, the empirical function of Reynolds number in turbulent model (cf. Eq. (7)), are used as suggested in the literature [1, 2, 36]:

$$f_\mu = \exp\left[-\frac{3.4}{(1 + Re_t/50)^2}\right] \quad (9a)$$

$$f_\mu = \exp\left[-\frac{2.5}{(1 + Re_t/50)}\right] \quad (9b)$$

$$f_\mu = 1. \quad (9c)$$

The latter form is the asymptotic value of f_μ as Re_t, the turbulent Reynolds number, goes to infinity; where:

$$Re_t = \frac{\varrho k^2}{\mu \varepsilon}. \quad (10)$$

2.1 *Near-wall models*

In order to accurately represent the behavior of the fluid flow and temperature near the wall, particularly in the viscous sublayer where the turbulent Reynolds number is small, temperatures, turbulent kinetic energies and dissipation rates are obtained by using the near-wall models described below.

2.1.1 Near-wall kinetic energy model

For the kinetic energy calculations, a slight variation of the previously suggested near-wall model has been used [4]. This variation is discussed in the Appendix. Here, only the basic assumptions used in the development of this model which will be later used in the near-wall temperature model are given.

(i) In the finite-difference solution procedure, the first near-wall node (node P) is chosen to lie outside of the viscous sublayer (Fig. 1a). The viscous sublayer thickness is estimated so that the viscous sublayer Reynolds number, Re_ε, is constant and equal to 20. The flow is assumed to be fully turbulent beyond the sublayer.

(ii) In the viscous sublayer, the mean velocity parallel to the wall is assumed to vary linearly with distance from the wall, and linearly with the logarithmic distance over the fully turbulent region near the wall.

1 The value of σ_ε is calculated from $\sigma_\varepsilon = \frac{\varkappa^2}{(C_2 - C_1)\sqrt{C_{\mu\infty}}}$ where $\varkappa$ is the von Karman constant equal to 0.4187 [7]

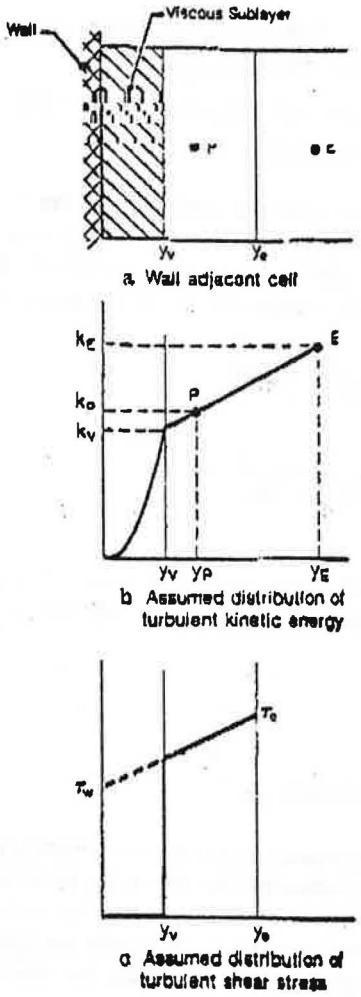

Fig. 1 a–c. Near-wall physical model

(iii) The variation of turbulent kinetic energy, k, is assumed to be parabolic in the viscous sublayer which corresponds to a linear increase of fluctuating velocity with distance from the wall, and linear over the remainder of the near-wall cell (Fig. 1 b).

(iv) The local turbulent shear stress is assumed to be piece-wise continuous; the stress is zero in the viscous sublayer and undergoes an abrupt increase at the edge of the sublayer and varies linearly over the remainder of the cell (Fig. 1 c).

(v) The dissipation rate, ε, in the viscous sublayer is shown to be constant and equal to $2\nu\left(\frac{\partial k^{1/2}}{\partial y}\right)^2$ [1]. In the fully turbulent region, ε is taken to vary linearly with $\frac{k^{3/2}}{y}$ [37].

2.1.2 Near-wall temperature model

As previously mentioned, the high-Reynolds-number form of the $k-\varepsilon$ model requires that the first node, in the finite-difference method of solution, be placed outside the viscous sublayer, resulting in a loss of detailed information close to the wall. The mean velocity and turbulent energy distributions are usually weakly dependent on the model of turbulent transport in the immediate vicinity of the wall [38]. However, this is not true for the heat transfer coefficient, which is highly sensitive to the choice of model to predict the near-wall temperature distribution. The dependence of fluid temperature on position is much stronger in the viscous sublayer than in the remainder of the near-wall cell. A model has been developed and incorporated into the energy equation to account for this variation. It should be noticed that the use of temperature model like the near-wall kinetic energy model is a direct consequence of finite difference approximation to the governing differential equations. In the near-wall temperature model, the quasi steady-state condition along with the averaged values for cross-flow velocity and streamwise temperature gradient are assumed.

The steady-state energy equation for incompressible flow near the wall can be expressed as:

$$u(y)\frac{\partial T}{\partial x}+v(x)\frac{\partial T}{\partial y}=\frac{\partial}{\partial y}\left[\left(\alpha+\frac{\mu_t}{\varrho\,\sigma_t}\right)\frac{\partial T}{\partial y}\right]. \tag{11}$$

Equation (11) assumes that the diffusion of heat in the direction of flow is small, and that the mean velocity in the main flow direction is a function of only the distance away from the wall (see assumption (ii)). Note that in Eq. (11) the secondary velocity, v, is a function of x only. This dependence is obtained by using the continuity equation with the assumption that the main flow velocity, u, in the near-wall cell depends only on y. To find the temperature variation in the near-wall cell ($y < y_p$), Eq. (11) is integrated from the wall ($y=0, T=T_w$) to the center of the near-wall cell ($y=y_p, T=T_p$) using the relation between the Nusselt number and the temperature derivative at the wall, i.e.,

$$Nu=\frac{2b}{T_b-T_w}\left.\frac{\partial T}{\partial y}\right|_w. \tag{12}$$

The resulting temperature distribution inside the near-wall cell is:

$$T-T_w=\int_0^y e^{-\int_0^y a(y)dy}\left[\int_0^y f(y)\,e^{\int_0^y a(y)dy}\,dy-\frac{T_w-T_b}{2b}Nu\right]dy \quad \text{for } y\leqq y_p. \tag{13}$$

The local Nusselt number can then be calculated by evaluating Eq. (13) at $y=y_p$; i.e.,

$$Nu=\frac{(T_w-T_P)/(T_w-T_b)+\psi}{\delta_{cor}} \tag{14}$$

where,

$$a(y)=\frac{\frac{1}{\varrho}\frac{\partial\mu_t}{\partial y}-v}{(\alpha+\mu_t/\varrho\,\sigma_t)} \tag{15a}$$

$$f(y) = -\frac{u(y)}{(\alpha + \mu_t/\varrho\,\sigma_t)}\frac{\partial T}{\partial x} \tag{15b}$$

$$\psi = \frac{1}{T_w - T_b}\left[\int_0^{y_p} e^{-\int a\,dy}\left(\int f e^{\int a\,dy}\right) dy\right] \tag{15c}$$

and

$$\delta_{cor} = \frac{1}{2b}\int_0^{y_p} e^{-\int a\,dy}\,dy. \tag{15d}$$

Note that with the assumptions used in the near-wall kinetic energy model, the effective turbulent viscosity, μ_t, is a function of the vertical position, y, which will be discussed in detail later. In the case of a fully developed temperature profile, ψ vanishes because the temperature does not vary in the flow direction, that is, $f = 0$ (cf. Eq. (15b)). In the cases where ψ is not zero, the local Nusselt number or heat transfer coefficient for the developing flow may be lower or higher than in the case of a fully developed temperature profile, depending on the sign of ψ. The sign of ψ depends on the variation of temperature in the flow direction as well as on the heat transfer process, that is, heating or cooling. The corrected distance, δ_{cor}, that accounts for the effect of eddy transport close to the wall in the near-wall cell, is used in calculating the heat transfer coefficient. Several special cases of interest can be obtained from Eqs. (14) and (15). Some of them are:

(i) fully developed velocity and temperature case;

$$\psi = 0 \tag{16a}$$

and

$$\delta_{cor} = \frac{1}{2b}\int_0^{y_p}\frac{dy}{\left[1 + \dfrac{Pr}{\sigma_t}\dfrac{\mu_t}{\mu}\right]} \tag{16b}$$

(ii) fully developed velocity case;

$$\psi = -\frac{1}{\alpha(T_w - T_b)}\frac{\partial T}{\partial x}\int_0^{y_p}\frac{\int u\,dy}{\left[1 + \dfrac{Pr}{\sigma_t}\dfrac{\mu_t}{\mu}\right]}dy \tag{17}$$

and δ_{cor} is given by Eq. (16b).

Equations (14) and (15) can be evaluated if the functional behavior of $u(y)$ and the effective turbulent viscosity, μ_t, are known in both the viscous and turbulent regions of the near-wall cell. To obtain the functional behavior of μ_t near the wall, the near-wall kinetic energy model assumptions are applied to the temperature model. For the flow across the channel, fully developed flow near the wall is assumed; i.e., $v = 0$. The variation of the viscosity is calculated as follows:

(i) Viscous sublayer:

The effective viscosity is calculated by substituting Eq. (A3) and Eq. (A8) into Eq. (6), which yields:

$$\mu_t = \tfrac{1}{2} C_\mu \frac{\varrho}{\gamma} k_r \frac{y^4}{y_v^2} \propto y^4. \tag{18}$$

The same proportionality given in Eq. (18) can also be found by using the Prandtl mixing length theory where the effective viscosity is calculated from [39]:

$$\mu_t = \varrho\, l_m^2 \left|\frac{\partial u}{\partial y}\right| \tag{19}$$

where the mixing length, l_m, is given by Van Driest's relation as

$$l_m = K y\left[1 - \exp\left(-\tau\varrho^{1/2} y/\mu A\right)\right] \tag{20}$$

K and A in Eq. (20) are empirical coefficients. For the case $y \ll 1$, Eq. (20) reduces to

$$l_m = K y\left[\tau\varrho^{1/2} y/\mu A\right] \propto y^2. \tag{21}$$

Assuming a linear variation of the main flow velocity near the wall and substituting Eq. (21) into Eq. (19) yields:

$$\mu_t \propto y^4 \tag{22}$$

which has the same proportionality as given in Eq. (18).

(ii) Fully turbulent region:

Substituting Eqs. (A3) and (A8) into the effective turbulent viscosity equation, Eq. (6) yields

$$\mu_t = C_\mu \varrho\, c_l y\left[k_P + \left(\frac{k_v - k_P}{y_v - y_P}\right)(y - y_P)\right]^{1/2} \quad \text{for } y_v \leqq y \leqq y_p. \tag{23}$$

Note that in Eq. (23), the value of the turbulent kinetic energy at the edge of the viscous sublayer is used instead of that calculated at node E.

In the fully turbulent region, the turbulent viscosity is calculated from Eq. (23). Equations (18) and (22) suggest that the turbulent viscosity in the viscous sublayer should vary with the fourth power of the distance from the wall. This variation is found by matching the effective viscosities at the edge of the viscous sublayer, which then yields.

$$\mu_t = C_\mu \varrho\, c_l y_v k_v^{1/2}(y/y_v)^4 \quad \text{for} \quad y \leqq y_v. \tag{24}$$

The integrals in Eqs. (15c) and (15d) can now be evaluated by splitting them into two parts, namely, viscous sublayer and fully turbulent region, and using the relations given in Eqs. (24) and (23) respectively.

3 Method of solution

The turbulence model described above has been incorporated into a numerical program previously developed for laminar convection [40]. The program is capable of handling both forced and free convection. The transport equations are solved using the Patankar-Spalding hybrid differencing scheme [41]. The time-dependent partial differential equations are integrated over a finite number of cells and over each time step. The resulting equations are modified for the near-wall cells as required by the near

wall models. The procedure results in a set of simultaneous algebraic equations that are solved iteratively for the velocity, temperature, pressure, turbulent kinetic energy, dissipation rate and turbulent viscosity profiles. The resulting temperature profile is then used to calculate the local heat transfer coefficients.

The steady-state solution to a given problem can be obtained either by solving the time dependent governing equations until the steady-state solution is reached or solving the steady-state equations iteratively. Using the time dependent equations has the advantage of converging the steady-state solution in complex flows (e.g. recirculating flows) with smaller time increments at the price of higher computation time. On the contrary, the iterative solution of the steady-state equations, in general, has convergence problems. However, if the solution converges it requires less computation time than the previous method. In non-recirculating flows (e.g. channel or pipe flows) it is found that the steady-state solution is obtained faster by using steady-state equations rather than the transient ones.

In the present work, the steady-state form of the governing equations has been used (the time dependent terms of the governing equations are dropped) to study the heat transfer and hydrodynamics of the channel flow. The fully developed experimental velocity profiles are used as the initial conditions for starting iteration.

The predictions of the computer program are assumed to have converged when the relative changes in quantities of interest between two successive iterations are less than 10^{-5}. The convergence is usually established within 2000 iterations. 20 grids are taken in the flow and cross flow directions. The grid sizes in the flow direction are based on the length of the channel. Uniform and non-uniform spacings are used in the flow and cross flow directions, respectively.

4 Results and discussion

Two-dimensional steady-state fully developed turbulent flow in a channel has been considered to study the sensitivity of predicted velocity, temperature, turbulent kinetic energy and effective turbulent viscosity profiles to the choice of constants used in the two-equation $k-\varepsilon$ model. Fluid flow between two parallel walls maintained at different constant temperatures has been analyzed. For the case of steady-state, fully developed velocity and temperature profiles, the same amount of heat transferred into the fluid from the hot wall is removed by the cold wall. Therefore, the problem may be also considered as a constant heat addition and removal process in a channel.

Most available experimental data pertain only to flow measurements, that is, velocity, shear stress, etc. These data include the earlier measurements of Laufer [20] and those of the recent works of Clark [21], Hussain and Reynolds [22], and El Telbany and Reynolds [23, 24]. The predictions of flow behavior are compared with the results of [20, 22]. Experimental data for temperature distribution in a fully developed channel flow are less common. The only detailed temperature data are those of Corcoran et al. [16, 17] and Page et al. [18, 19]; both have been used for comparisons presented below. The predictions of heat transfer coefficients are also compared to available correlations and experimental data.

Due to the important role of the effective turbulent viscosity in the governing equations, a number of variations in the $k-\varepsilon$ model constants have been used in performing comparisons with the experimental data. The five cases employed in this sensitivity study are shown in Table 1. In the first three cases, only the coefficient of turbulent viscosity, C_μ, has been varied. The first variation is the asymptotic value of C_μ as the turbulent Reynolds number goes to infinity (cf. Eq. (9c)) [1, 2, 36], and for the next two variations it is taken to be a function of the turbulent Reynolds number (cf. Eqs. (9a) and (9b)). In the fourth case, in addition to the variation of the coefficient of turbulent viscosity (case 3), the coefficients in the logarithmic velocity profile used in the near-wall kinetic energy model (cf. Eq. (A1)) are altered to be consistent with experimentally correlated values. In the last variation, case 5, the turbulent kinetic energy Prandtl number, σ_k is changed.

Each of these five cases has been used in the analysis with and without the near-wall temperature model. Since the energy equation is decoupled from the other equations, the flow predictions are not affected by the inclusion of the near-wall temperature model.

The velocity predictions of the model are compared to the experimental data of Laufer [20] (Fig. 2a), Hussain and Reynolds [22] (Fig. 2b) and Page et al. [18, 19] (Fig. 2c). From Figs. 2a–c, it is seen that the velocity predictions are insensitive to variation of the constants in the $k-\varepsilon$ model. All of the cases (Table 1) predict the velocity profile very well compared to the experimental data. If the ultimate goal was to predict only the velocity profile, then the constants suggested in the literature [1–4] could be used without introducing significant error in the predictions. However, as will be shown, this conclusion is not true for the predictions of the other dependent variables.

Table 1. The variations used in the sensitivity study[a]

Case 1	$C_\mu = 0.09$
Case 2	$C_\mu = 0.09 \exp[-2.5/(1+Re_t/50)]$
Case 3	$C_\mu = 0.09 \exp[-3.4/(1+Re_t/50)^2]$
Case 4	Case 3 with the experimental values of the constants in the logarithmic velocity profile, Eq. (11)
Case 5	Case 3 with $\sigma_k = 1.255$

[a] The profiles labeled with primes in the accompanying figures correspond to the cases without near-wall temperature model

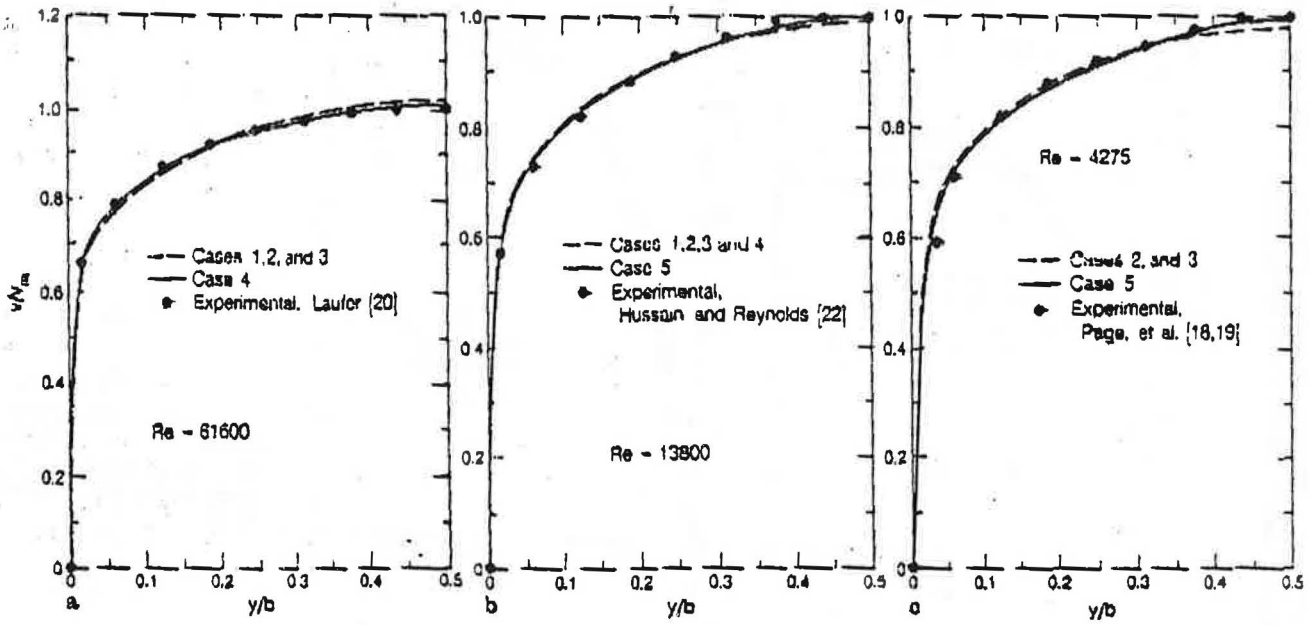

Fig. 2 a – c. a Comparison of the predicted velocity profiles with the measurements of Laufer [20] at $Re = 61\,600$; b Comparison of the predicted velocity profiles with the measurements of Hussain and Reynolds [22] at $Re = 13\,800$; c Comparison of the predicted velocity profiles with the measurements of Page et al. [18, 19] at $Re = 4275$

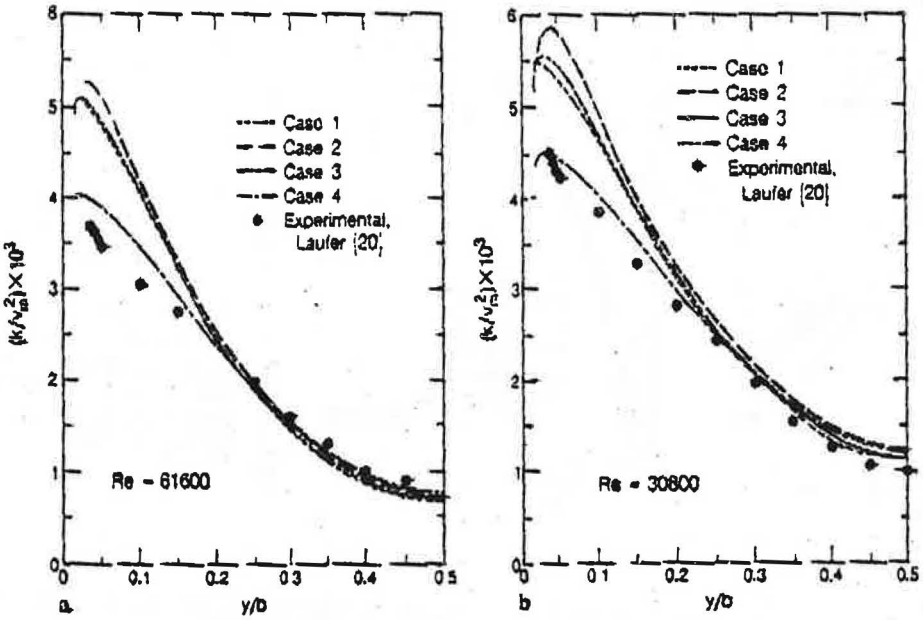

Fig. 3. a Comparison of the predicted turbulent kinetic energy profiles with the measurements of Laufer [20] at $Re = 61\,600$; b Comparison of the predicted turbulent kinetic energy profiles with the measurements of Laufer [20] at $Re = 30\,800$

The calculated turbulent kinetic energy for the first four cases is compared to the experimental data of Laufer [20] for two different Reynolds numbers in Figs. 3a ($Re = 61\,600$) and 3b ($Re = 30\,800$). The predictions of the turbulent kinetic energy near the wall are seen to be highly sensitive to the choice of constants. When the effective turbulent viscosity coefficient is combined with the experimentally calculated values of the constants in the logarithmic velocity profile near the wall (case 4), the predictions of the model are noticeable improved.

The calculated turbulent viscosity for the first four cases identified in Table 1 is compared in Fig. 4a and 4b. The results indicate that the constants used in the calculation of the velocity and turbulent kinetic energy profiles can be adjusted to provide an accurate representation of the turbulent viscosity close to the wall. The effect of these adjustments on the distribution of the turbulent viscosity toward the center of the channel is not sufficient enough to reproduce the experimentally observed characteristics. Experimental evidence indicates that the effective turbu-

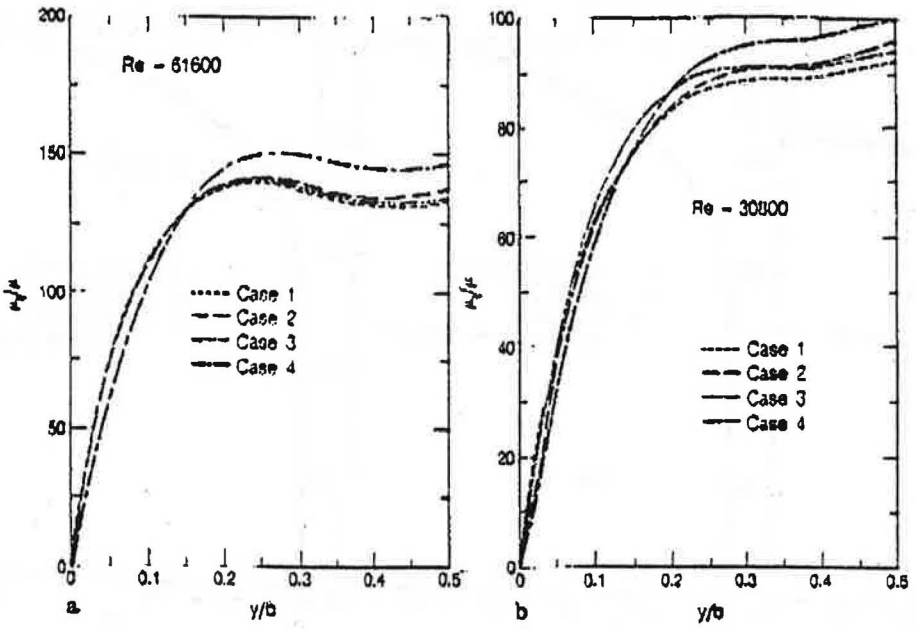

Fig. 4. a Predicted variation of turbulent effective viscosity across the channel at $Re = 61\,600$; b Predicted variation of turbulent effective viscosity across the channel at $Re = 30\,800$

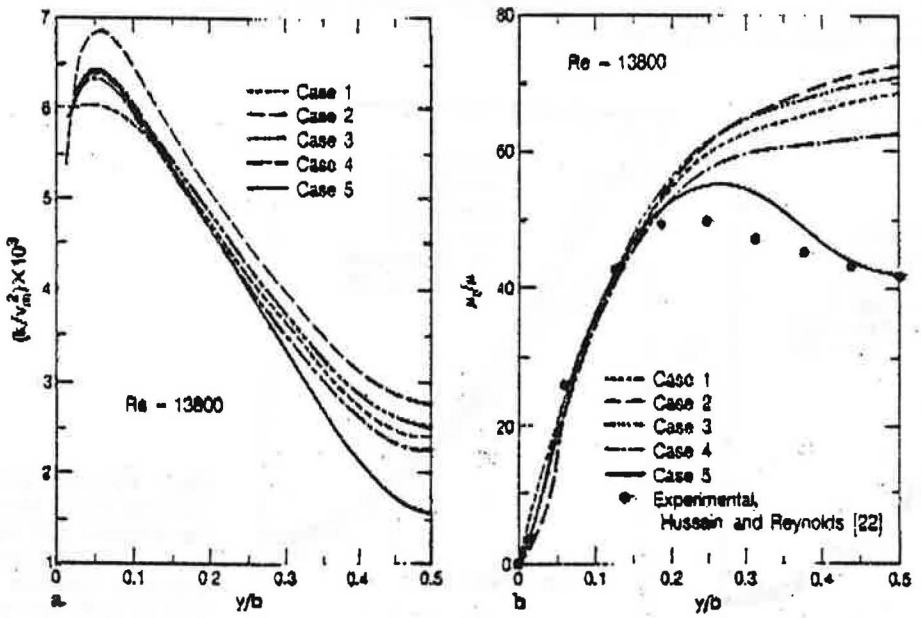

Fig. 5. a Predicted variation of turbulent kinetic energy at $Re = 13\,800$; b Comparison of the predicted effective turbulent viscosity to the experimental data of Hussain and Reynolds [22] at $Re = 13\,800$

lent viscosity increases with distance from the wall, reaches a maximum and then decreases to a value of about 0.7 times the product of the friction velocity and the boundary layer thickness near the center of the channel or pipe [22]. The effective viscosity variations calculated by using the suggested coefficients [1–4] for the above mentioned cases do not demonstrate this same behavior (Figs. 4a and 4b). At high-Reynolds-number flows, the turbulent viscosities near the center of the channel are so high that variations in viscosity in that region would not significantly affect the flow and heat transfer calculations. However, for low-Reynolds-number flow, a small variation in viscosity in the region close to the center would have a significant effect in these calculations.

In order to predict an effective turbulent viscosity near the center of the channel that is consistent with the experiments, the turbulent kinetic energy Prandtl number, σ_k, can also be adjusted. Although this does not result in a significant change in the prediction of turbulent kinetic energy and turbulent viscosity close to the wall, it does affect the predictions of these quantities toward the center of the channel as is shown in Figs. 5a and b. The predictions of the turbulent viscosities are compared to the experimental data of Hussain and Reynolds [22] in Fig. 5b

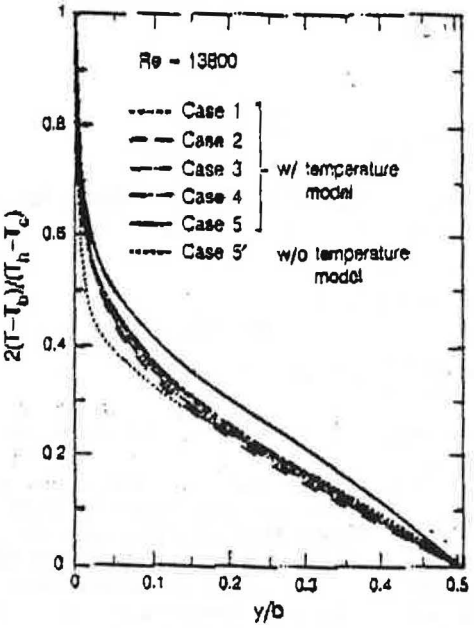

Fig. 6. Comparison of the predicted temperature profiles with and without near-wall temperature model at $Re = 13800$

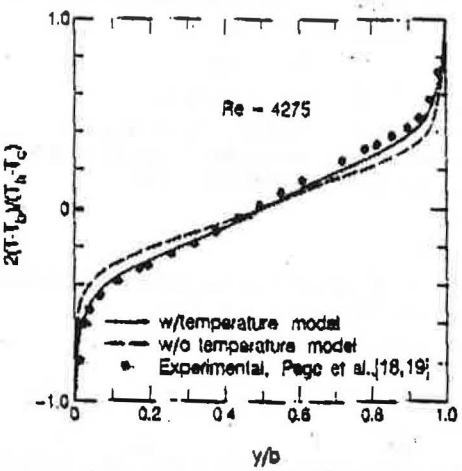

Fig. 7. Comparison of the predicted temperature profiles with and without near-wall temperature model to the experimental data of Page et al. [18, 19] at $Re = 4275$

which shows a substantial improvement of case 5 over the other four cases.

As discussed in conjunction with the description of the near-wall temperature model, the effective turbulent viscosity plays an important role in the prediction of the temperature profile and therefore, local heat transfer coefficients. The predicted temperature profiles, for the flow conditions studied by Hussain and Reynolds [22], are shown in Fig. 6. In obtaining these temperature profiles, the near-wall temperature model was incorporated into the analysis. In addition, the calculations were repeated for the same constants as used with case 5, but without the near-wall temperature model; the results are shown as case

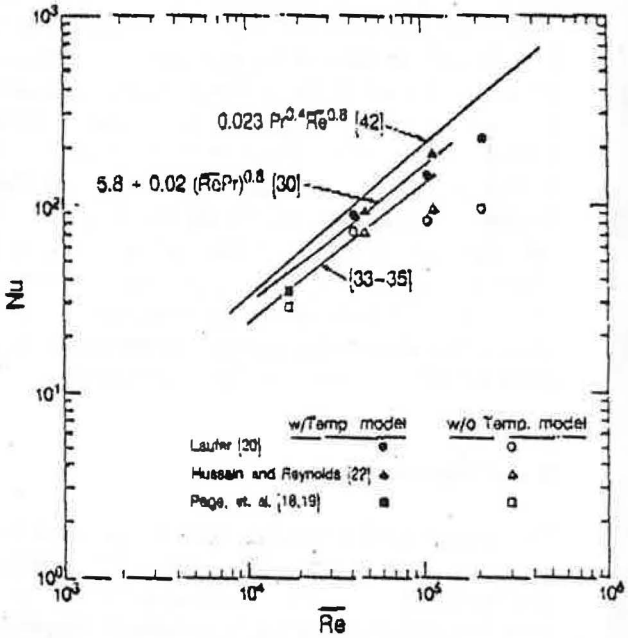

Fig. 8. Comparison of the predicted Nusselt number with and without near-wall temperature models

5'. Comparing the results labeled as case 5 and case 5', one observes that the near-wall temperature model produces smaller temperature gradient in the near-wall region.

Calculated temperature profiles are compared to the data of Page et al. [18, 19] in Fig. 7. The profiles are obtained by using the experimental values of turbulent viscosity in the calculations. Comparison of the results with the experimental data indicates that the calculated temperature profile, especially near the boundary, is noticeably improved by use of the near-wall temperature model. This is especially important since near the boundary the temperature gradient plays a significant role in the calculation of the heat transfer coefficient.

The prediction of the Nusselt number with the $k-\varepsilon$ model has been greatly improved by including the near-wall temperature model, as shown in Fig. 8. The results are compared to the correlations of Dittus-Boelter [42] (for pipe flow) and of Seban [30] (for asymmetrically heated walls) and the calculations of Barrow [33–35]. It is observed by Levy et al. [26] that the heat transfer coefficients predicted by the Dittus-Boelter correlation for a symmetrically heated channel are 15–30 percent higher than the experimental values. Barrow [33–35] and Sparrow et al. [27] also showed that the heat transfer coefficients for asymmetrically heated walls (as in the present study of one heated and one cold wall) are even smaller than those of the symmetrically heated channel.

The Nusselt number predictions with the near-wall temperature model are in good agreement with the results of Seban [30] and Barrow [33–35]. Also, the predicted Nusselt numbers are about 15–30 percent lower than the predictions of pipe flow equation [42] which are in

agreement with the experimental observations of Levy et al. [26] and Sparrow et al. [27]. Predictions of the Nusselt number without the near-wall temperature model are also presented in Fig. 8. Nusselt numbers calculated in this way are much lower than either the theoretical or experimental results. The deviation from the experimental and theoretical values increases as the Reynolds number increases; this can be attributed to the choice of the high-Reynolds-number form of the $k-\varepsilon$ model, in which the near-wall kinetic energy model requires that the first node be outside the viscous sublayer. Therefore, the predictions without the near-wall temperature model become less accurate at higher Reynolds numbers.

5 Conclusions

The high-Reynolds-number form of the $k-\varepsilon$ model as modified by the near-wall turbulent kinetic energy model has been applied to a fully developed channel flow. It has been found that the model with constants suggested in the literature does not predict the correct variation of the effective turbulent viscosity away from the wall, which in turn affects the prediction of temperature distribution and local heat transfer coefficients. In order to predict the correct behavior of the turbulent viscosity toward the center of the channel, the turbulent kinetic energy Prandtl number, σ_k, has to be adjusted for the flow conditions which suggests that this quantity should be a function of Reynolds number.

The $k-\varepsilon$ model modified solely by the near-wall kinetic energy model does not predict the temperature profile and local heat transfer coefficients accurately, and its predictions become less accurate as the Reynolds number increases. A near-wall temperature model, similar to the near-wall turbulent kinetic energy model, has been developed to improve the prediction of the $k-\varepsilon$ turbulent model. Limited comparisons of the predicted results with experimental data and available correlations show a good agreement.

Acknowledgement

This work was supported by the Assistant Secretary for Conservation and Renewable Energy, Office of Solar Heat Technologies, Passive and Hybrid Solar Energy Division, of the U.S. Department of Energy under Contract No. DE-AC03-76SF00098.

Appendix

Description of the near-wall kinetic energy model

The near-wall kinetic energy model described in [4] is as follows: Based on the assumptions stated in the text, the mean velocity parallel to the wall and the turbulent kinetic energy are given as:

a) velocity,

$$u=\begin{cases}\dfrac{\tau_w}{\varrho\nu}y & \text{for } y\le y_v\\ \dfrac{\tau_w}{\varkappa C_\mu^{1/4}\varrho k_v^{1/2}}\ln\left(E^*\dfrac{y k_v^{1/2}}{\nu}\right) & \text{for } y_v\le y\le y_e.\end{cases}\tag{A1}$$

where the continuity of the velocity at the edge of the viscous sublayer requires that the constant E^* be given by

$$E^*=\exp(\varkappa C_\mu^{1/4} Re_v)/Re_v.\tag{A2}$$

b) turbulent kinetic energy,

$$k=\begin{cases}k_v(y/y_v)^2 & \text{for } y\le y_v\\ k_P+\dfrac{k_E-k_P}{y_E-y_P}(y-y_P) & \text{for } y_v\le y\le y_e\end{cases}\tag{A3}$$

where k_v is obtained by evaluating Eq. (A3) at the edge of the viscous sublayer.

The local turbulent shear stress distribution, τ_t, over the near-wall cell, is necessary in order to determine the mean rate of kinetic energy production. Physically in the region close to the wall where turbulent eddies are infrequently present, the local turbulent shear stress is taken as zero. This stress increases rapidly in a short distance outside the laminar layer. For computation purposes, the laminar sublayer and the short transition region are combined in a single region as the viscous sublayer. Therefore, the local turbulent shear stress is assumed to be piece-wise continuous; the stress is zero in the viscous sublayer and undergoes an abrupt increase at the edge of the sublayer and varies linearly over the remainder of the cell (Fig. 1c).

$$\tau_t=\begin{cases}0 & \text{for } y<y_v\\ \tau_w+(\tau_e-\tau_w)y/y_e & \text{for } y_v\le y\le y_e\end{cases}\tag{A4}$$

where τ_w is calculated by evaluating Eq. (A1) at node P.

The mean rate of production of kinetic energy per unit volume can then be evaluated by integrating

$$\tau_t\left(\frac{\partial u}{\partial y}+\frac{\partial r}{\partial x}\right)\tag{A5}$$

over the surface of the cell with the aforementioned assumptions. The final form of the equation is given as:

Mean production rate

$$=\frac{\tau_w^2}{\varkappa C_\mu^{1/4}\varrho k_v^{1/2}y_e}[\ln(y_v/y_v)+(\tau_e/\tau_w-1)(1-y_v/y_e)]+\tau_w\frac{\partial r}{\partial x}(1-y_v/y_e)+\tfrac{1}{2}(\tau_e-\tau_w)\frac{\partial r}{\partial x}[1-(y_v/y_e)^2].\tag{A6}$$

Equation (A6) is different from the one used in Ref. [4]. Equation (A6) may also be written in terms of u_e and u_v (the form given in Ref. [4]) by using the logarithmic velocity profile, Eq. (A1):

Mean production rate

$$=\frac{\tau_w(u_v-u_e)}{y_e}+\frac{\tau_w(\tau_e-\tau_w)}{\varrho\varkappa^* k_v^{1/2}y_e}(1-y_v/y_e)+\tau_w\frac{\partial r}{\partial x}(1-y_v/y_e)+\tfrac{1}{2}(\tau_e-\tau_w)\frac{\partial r}{\partial x}[1-(y_v/y_e)^2].\tag{A7}$$

Equation (A6) resulted from the integration of the production term over the near-wall cell; therefore, it assures that the production term is always positive (this could also be proved by expansion of Eq. (A6)). Equation (A7), however, is derived by changing the variables in the first part of Eq. (A6) to the velocity variables. The velocities are calculated during the iteration process, and do not necessarily vary logarithmically over the near-wall cell. Therefore, the use of Eq. (A7) could result in a negative overall production rate.

The negative production rate in one near-wall cell would result in a change in the kinetic energy and, consequently, in a higher production term in the adjacent near-wall cell to compensate for the error of the previous near-wall cell. This process would yield a stable periodic oscillation of the turbulent kinetic energy along the flow direction. To overcome this periodic oscillation, the use of Eq. (A6) rather than Eq. (A7) is recommended.

As it was mentioned in the assumption (v) given in the text, the dissipation rate, ε, in the viscous sublayer is shown to be constant and equal to $2\nu\left(\frac{\partial k^{1/2}}{\partial y}\right)^2$ [1]. This constant value is evaluated by using the assumed turbulent kinetic energy profile in the viscous sublayer (cf. Eq. (A3)). In the fully turbulent region, ε is taken to vary linearly with $\frac{k^{3/2}}{y}$ [37].

$$\varepsilon = \begin{cases} 2\nu k_r/y_r^2 & \text{for } y < y_r \\ k^{3/2}/c_l y & \text{for } y_r \le y \le y_r \end{cases} \tag{A8}$$

where c_l is a constant equal to 2.55.

In the derivation of Eq. (A8), the parabolic assumption of turbulent kinetic energy in the viscous sublayer is used to evaluate the constant value of the dissipation rate (cf. Eq. (A3)).

The mean dissipation rate for the cell, $\bar{\varepsilon}$, can now be evaluated by integrating Eq. (A8) over the near-wall cell. The resulting equation is given in Ref. [4].

References

1. Jones, W. P.; Launder, B. E.: The prediction of laminarization with a two-equation model of turbulence. Int. J. Heat Mass Transfer 15 (1972) 301–314
2. Jones, W. P.; Launder, B. E.: The calculation of low-Reynolds-number phenomena with a two-equation model of turbulence. Int. J. Heat Mass Transfer 16 (1973) 1119–1130
3. Launder, B. E.; Spalding, D. B.: The numerical computation of turbulent flows. Computer Methods in Applied Mechanics and Engineering 3 (1974) 269–289
4. Chieng, C. C.; Launder, B. E.: On the calculation of turbulent heat transport downstream from an abrupt pipe expansion. Numerical Heat Transfer 3 (1980) 189–207
5. Amano, R. S.: Development of a turbulence near-wall model and its application to separated and reattached flows. Numerical Heat Transfer 7 (1984) 59–75
6. Johnson, R. W.; Launder, B. E.: Discussion of: On the calculation of turbulent heat transport downstream from an abrupt pipe expansion. Numerical Heat Transfer 5 (1982) 493–496
7. Sindir, M. M.: Numerical study of turbulent flows in backward-facing step geometries: Comparison of four models of turbulence. Ph.D. Thesis, Mechanical Engineering Department, Univ. of Calif., Davis, 1982
8. Sindir, M. M.: Effects of Expansion ratio on the calculation of parallel-walled backward-facing step flows: Comparison of four models of turbulence. ASME Paper No. 83-FE-10, 1983
9. Sindir, M. M.: Calculation of deflected-walled backward-facing step flows: Effects of angle of deflection on the performance of four models of turbulence. ASME Paper No. 83-FE-16, 1983
10. Sindir, M. M.; Harsha, P. T.: Assessment of turbulence models for scramjet flowfields. NASA Contractor Report 3643, November 1982
11. Humphrey, J. A. C.; Pouruhmadi, F.: A generalized algebraic relation for predicting developing curved channel flow with a $k-\varepsilon$ model of turbulence. 3rd symposium on turbulent shear flow. Univ. of Calif., Davis, 1983 (also Lawrence Berkeley Laboratory Report, LBL-12009)
12. Humphrey, J. A. C.; Chang, S. M.: Turbulent flow in passage around a 180° bend: An experimental and numerical study. Univ. of Calif. Berkeley, Rep. FM-83-7, 1983
13. Naot, D.; Rodi, W.: Calculation of secondary currents in channel flow. ASCE J. Hydraulics Division 108 (1982) 948–968
14. Rodi, W.: Turbulence models and their application in hydraulics – a state of the art review. Univ. Karlsruhe Report. SFB 80/T/127, Fed. Rep. Germany, 1978
15. Washington, L.; Marks, W. M.: Heat transfer and pressure drop in rectangular air passages. Ind. and Eng. Chem. 29 (1937) 337–345
16. Corcoran, W. H.; Roudebush, B.; Sage, B. H.: Temperature gradients in turbulent gas streams: Preliminary studies. Chem. Eng. Prog. 43 (1947) 135–142
17. Corcoran, W. H.; Page, F., Jr.; Schlinger, W. H.; Sage, B. H.: Temperature gradients in turbulent gas streams: Methods and apparatus for flow between parallel plates. Ind. and Eng. Chem. 44 (1952) 410–419
18. Page, F., Jr.; Corcoran, W. H.; Schlinger, W. G.; Sage, B. H.: Temperature gradients in turbulent gas streams: Temperature and velocity distributions in uniform flow between parallel plates. Ind. Eng. Chem. 44 (1952) 419–424
19. Page, F., Jr.; Schlinger, W. G.; Breaux, D. K.; Sage, B. H.: Temperature gradients in turbulent gas streams: Point values of eddy conductivity and viscosity in uniform flow between parallel plates. Ind. Eng. Chem. 44 (1952) 424–430
20. Laufer, J.: Investigation of turbulent flow in a two-dimensional channel. NACA Technical Note 2123, 1950
21. Clark, J. A.: A study of incompressible turbulent boundary layers in channel flow. ASME J. Basic Eng. 90 (1968) 455–468
22. Hussain, A. K. M. F.; Reynolds, W. C.: Measurement of fully developed turbulent channel flow. ASME J. Fluids Eng. 97 (1975) 568–580
23. El Telbany, M. M. M.; Reynolds, A. J.: Velocity distributions in plane turbulent channel flows. J. Fluid Mech. 100 (1980) 1–29
24. El Telbany, M. M. M.; Reynolds, A. J.: Turbulence in plane channel flows. J. Fluid Mech. 111 (1981) 283–318
25. Lancet, R. T.: The effect of surface roughness on the convection heat-transfer coefficient for fully developed turbulent flow in ducts with uniform heat flux. ASME J. Heat Transfer 81 (1959) 168–174
26. Levy, S.; Fuller, R. A.; Niemi, R. O.: Heat transfer to water in thin rectangular channels. ASME J. Heat Transfer 81 (1959) 129–143
27. Sparrow, E. M.; Lloyd, J. R.; Hixon, C. W.: Experiments on turbulent heat transfer in an asymmetrically heated rectangular duct. ASME J. Heat Transfer 88 (1966) 170–174
28. Martinelli, R. C.: Heat transfer to molten metals. Trans. ASME 69 (1947) 947–960
29. Harrison, W. B.; Menke, J. R.: Heat transfer to liquid metals flowing in asymmetrically heated channels. Trans. ASME 71 (1949) 797–803
30. Seban, R. A.: Heat transfer to a fluid flowing turbulently between parallel walls with asymmetric wall temperatures. Trans. ASME 72 (1950) 789–795
31. Hatton, A. P.; Quarmby, A.: The effect of axially varying and unsymmetrical boundary conditions on heat transfer with turbulent flow between parallel plates. Int. J. Heat Mass Transfer 6 (1963) 903–914
32. Hatton, A. P.; Quarmby, A.; Grundy, I.: Further calculations on the heat transfer with turbulent flow between parallel plates. Int. J. Heat Mass Transfer 7 (1964) 817–823
33. Barrow, H.: Convection heat transfer coefficients for turbulent flow between parallel plates with unequal heat fluxes. Int. J. Heat Mass Transfer 1 (1961) 306–311

34. Barrow, H.: An analytical and experimental study of turbulent gas flow between two smooth parallel walls with unequal heat fluxes. Int. J. Heat Mass Transfer 5 (1962) 469–487
35. Barrow, H.; Lee, Y.: Heat transfer with unsymmetrical thermal boundary conditions. Int. J. Heat Mass Transfer 7 (1964) 580–582
36. Launder, B. E.; Sharma, B. I.: Application of the energy-dissipation model of turbulence to the calculation of flow near a spinning disc. Letters in Heat and Mass Transfer 1 (1974) 131–138
37. Spalding, D. B.: Heat transfer from turbulent separated flows. J. Fluid Mechanics 27 (1967) 97–109
38. Pope, S. B.; Whitelaw, J. H.: The circulation of near-wake flows. J. Fluid Mech. 73 (1976) 9–32
39. Launder, B. E.; Spalding, D. B.: Lectures in mathematical models of turbulence. New York: Academic Press 1972
40. Gadgil, A.: On convective heat transfer in building energy analyses. Ph.D. Thesis, Department of Physics. Univ. of Calif., Berkeley, 1979 (also Lawrence Berkeley Laboratory Report, LBL-10900)
41. Patankar, S. V.; Spalding, D. B.: Heat and Mass Transfer in Boundary Layers. London: Morgan-Grampion 1967
42. Maurer, G. W.; Le Tourneau, B. W.: Friction factors for fully developed turbulent flow in ducts with and without heat transfer. ASME J. Basic Eng. 86 (1964) 627–636

Hashem Akbari
Atila Mertol
Ashok Gadgil
Ron Kammerud
Fred Bauman
Passive Research and Development Group
Lawrence Berkeley Laboratory
University of California
Berkeley, California 94720
USA

Received November 2, 1984